Available online at www.sciencedirect.com

Journal of the European Ceramic Society 24 (2004) 2689–2697

www.elsevier.com/locate/jeurceramsoc

A comparative study of the thermal transformations of Ba-exchanged zeolites A, X and LSX

S. Esposito[a], C. Ferone[a], M. Pansini[a,*], L. Bonaccorsi[b], E. Proverbio[b]

[a]Laboratorio Materiali del Dipartimento di Meccanica, Strutture, Ambiente e Territorio, Facoltà di Ingegneria dell'Università di Cassino, Via G. Di Biasio 43, 03043 Cassino (Fr), Italy

[b]Dipartimento di Chimica Industriale e Ingegneria dei Materiali, Università di Messina, Salita Sperone 31- S. Agata di Messina, 98166 Messina, Italy

Received 23 March 2003; received in revised form 15 September 2003; accepted 20 September 2003

Abstract

In this investigation samples of exhaustively Ba-exchanged zeolites Ba–A, Ba–X, and Ba–LSX were subjected to thermal treatments in the temperature range 200–1550 °C for times up to 40 h. Their thermal transformations were comparatively studied by room temperature X-ray diffraction. Upon heating, the three zeolites undergo the following sequence of transformations: zeolite→amorphous phase→hexacelsian→monoclinic celsian in strongly different ways. In particular it was found that: (1) The crystallisation of nuclei of monoclinic celsian dispersed in the amorphous phase arising from the thermal collapse of the structure of zeolite Ba–A, recorded above 500 °C in a previous work, did not occur for zeolites Ba–X and Ba–LSX. (2) Zeolite Ba–A exhibited a far greater reactivity than zeolites Ba–X and Ba–LSX; actually, the conversion of hexacelsian into monoclinic celsian attained completion at 1300 °C, starting from zeolite Ba–A, whereas did not attain completion in the most severe experimental conditions experienced (1550 °C, 24 h), starting from zeolites Ba–X and Ba–LSX. Such different thermal behaviours could be reasonably ascribed to the different middle-range order occurring in the amorphous phases arising from the thermal collapse of the microporous structures of zeolites Ba–A, Ba–X, and Ba–LSX.

Keywords: Celsian; Powders-solid state reaction; Silicates; X-ray methods

1. Introduction

The scientific and technological community exhibits great interest towards the monoclinic polymorph of barium feldspar celsian ($BaAl_2Si_2O_8$) owing to its remarkable thermal and electrical properties.[1]

The essential literature concerning the synthesis of celsian, which was reviewed in previous papers,[2,3] reports that the occurrence of several drawbacks makes it quite difficult and expensive. Among these drawbacks the high temperatures and/or long reaction times of thermal treatments,[2,3] the use of alkoxides[4] or the set up of complex reacting systems,[5] may be cited. Moreover most of the reported procedures of synthesis of celsian lead to the crystallisation of the hexagonal polymorph of celsian (hexacelsian). Actually it is the first polymorph to nucleate on account of the simpler crystal structure of the high-symmetry modification presenting a lower kinetic barrier to nucleation,[6] even though it is stable at temperatures higher than 1590 °C.[7]

A long term study[2,3,8,9] concerning the thermal transformation of Ba-exchanged zeolites into monoclinic celsian was undertaken. This study started from the work of Subramanian and coworkers[10–13] who crystallised alkaline-earth and alkaline framework aluminosilicates, which belong to the class of the feldspars, by thermal treatment of cation exchanged zeolites at temperatures slightly higher than 1000 °C for some hours. Very interesting results were obtained in this study. In particular it was found that, upon a thermal treatment at temperatures higher than 1000 °C, Ba-exchanged zeolite A, which after dehydration exactly reproduces the stoichiometric composition of celsian, gave rise to the following sequence of transformations: zeolite→amorphous

---

* Corresponding author. Tel.: +39-0776-299717; fax: +39-0776-299711.

E-mail address: pansini@unicas.it (M. Pansini).

0955-2219/$ - see front matter © 2003 Elsevier Ltd. All rights reserved.
doi:10.1016/j.jeurceramsoc.2003.09.017

phase→hexacelsian→monoclinic celsian. Moreover it was found that 6 h at 1100 °C or 22 h at 1300 °C were sufficient to transform samples of Ba-exchanged zeolite A, containing 0.58 and 0.20 meq/g Na residual amount, respectively, into fully monoclinic celsian.[2,3] Nevertheless the reactivity of the system appears strongly affected even by parameters other than Na residual amount.[2,3] Actually Ba-exchanged zeolite X was found to totally convert into monoclinic celsian by thermal treatment at 1550 °C for 24 h. This result was reported by Hoghooghi and coworkers,[14] and in ref. 2 for Ba-exchanged zeolite X samples bearing 0.61 and 0.26 meq/g Na residual amount, respectively.

These considerations promoted the present work in which samples of commercial A, commercial X and laboratory synthesised LSX zeolites were previously subjected to exhaustive Ba-exchange. These zeolites were chosen inasmuch as commercial A and laboratory synthesised LSX zeolites exhibit about the same chemical composition and Si/Al ratio (1.00 and 1.02, respectively) but different structures (Fig. 1),[15] whereas commercial X and laboratory synthesised LSX zeolites exhibit the same structure[15] but different Si/Al ratios (1.23 and 1.02, respectively). Subsequently the phenomena occurring thermally treating these zeolites at temperatures ranging from 200 to 1550 °C for times up to 40 h are investigated. The comparative study of the thermal transformations of these zeolites should allow a better comprehension of the mechanisms of the reactions leading to monoclinic celsian.

2. Experimental

Carlo Erba reagent-grade synthetic zeolites 4A ($Na_{12}Al_{12}Si_{12}O_{48}27H_2O$) and 13X ($Na_{86}Al_{86}Si_{106}O_{384}264H_2O$) were used. Zeolite LSX was synthesised in laboratory starting from a synthesis batch of the following composition: $5.5Na_2O{:}1.65K_2O{:}2.2SiO_2{:}1Al_2O_3{:}122H_2O$. This batch was obtained according to the following procedure: (1) Reagent grade Riedel-de-Haen hydrate alumina (Al_2O_3 65%) was dissolved in a NaOH solution prepared by dissolving Reagent grade Carlo Erba NaOH in bidistilled water. (2) Reagent grade Carlo Erba KOH was added to this solution. (3) Reagent grade BHD sodium silicate aqueous solution (SiO_2: 27.5%, Na_2O 8.0%) was added to this solution. This batch was kept at 70 °C for 3 h and then at 95 °C for 2 h under autogeneous pressure and continuous stirring. The final product was recovered by vacuum filtration, abundantly washed with bidistilled water, dried at 75 °C for 24 h and stored for at least 3 days in an environment having about 50% relative humidity to allow water saturation. The chemical formula of the synthesized LSX zeolite, determined through the chemical analysis, turned out: $Na_{73}K_{22}Al_{95}Si_{97}O_{384}212H_2O$. These three materials will be identified from this point onward as zeolites Na–A, Na–X and (Na, K)–LSX, respectively.

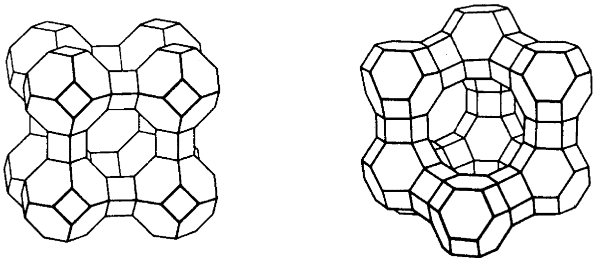

Fig. 1. Structures of zeolites A, X and LSX.

These zeolites were subjected to exhaustive Ba-exchange. Exchange operations, which were terminated when their iteration did not give rise to a sensible decrease of the alkaline cations residual amount, were performed as follows.

Zeolite Na–A was contacted with a warm (60–70 °C) $Ba^{2+} = 0.2$ N solution with a weight solid/liquid ratio $(S/L) = 1/25$. The solution was prepared using bidistilled water and Carlo Erba reagent-grade $Ba(NO_3)_2$ (purity 99.5%). The solid was separated from the liquid through filtration and again contacted with the exchange solution for a total of four times. Then a fifth exchange was performed at a weight $S/L = 1/50$, all other conditions being equal to previous ones. The remaining exchange operations were performed contacting the zeolite with barium solutions prepared using extremely pure $BaCl_2$ (purity >99.999%), provided by Aldrich. In particular a sixth exchange was performed at a weight $S/L = 1/20$ and $Ba^{2+} = 0.5$ g/dm^3, a seventh at a weight $S/L = 1/30$ and $Ba^{2+} = 7.5$ g/dm^3, and an eighth at a weight $S/L = 1/40$ and $Ba^{2+} = 7.5$ g/dm^3, all other conditions being equal to the previous ones.

Zeolite Na–X was contacted with a warm (60–70 °C) $Ba^{2+} = 0.5$ N solution with a weight solid/liquid ratio $(S/L) = 1/25$. The solution was prepared using bidistilled water and Carlo Erba reagent-grade $Ba(NO_3)_2$ (purity 99.5%). The solid was separated from the liquid through filtration and again contacted with the exchange solution for a total of four times. Then a fifth exchange was performed using a $Ba^{2+} = 0.2$ N solution, all other conditions being equal to previous ones.

Zeolite (Na, K)–LSX was contacted with a warm (60–70 °C) $Ba^{2+} = 0.2$ N solution with a weight solid/liquid ratio $(S/L) = 1/25$. The solution was prepared using bidistilled water and Carlo Erba reagent-grade $Ba(NO_3)_2$ (purity 99.5%). The solid was separated from the liquid through filtration and again contacted with the exchange solution for a total of seven times.

The duration time of each exchange ranged between 12 and 18 h and the initial pH of Ba^{2+} solutions used for the exchanges is about 5.8. The three materials obtained according to these procedures will be identified from this point onward as zeolites Ba–A, Ba–X and Ba–LSX, respectively.

The residual Na content of zeolites Ba–A, Ba–X and Ba–LSX and residual K content of zeolite Ba–LSX were determined according to the following procedure. The zeolite was chemically dissolved in a hydrofluoric and perchloric acid solution and its Na^+ and K^+ (in the case of zeolite Ba–LSX) concentration was determined by atomic absorption spectrophotometry (AAS), using a Perkin-Elmer Analyst 100 apparatus. The consistency of concentration measurements related to cation exchange operations was checked by determining Ba^{2+} concentration by titration with EDTA using erio T as the indicator and a NH_3 and NH_4^+ solution at pH 10 as buffer.[16]

The resulting powders were washed with bidistilled water, dried for about 1 day at 80 °C and stored for at least 3 days in an environment having about 50% relative humidity to allow water saturation of zeolites.

Table 1
Thermal treatments to which the various Ba-exchanged zeolite samples were subjected and figures where the corresponding XRD patterns are reported

Temp (°C)	Thermal treatment[a]
Zeolite A	
200	Q, 2 h (Fig. 2)
300	Q
400	Q
500	Q (Fig. 2)
600	Q
700	Q, 1 h, 4 h, 28 h
800	Q, 1 h, 4 h, 28 h (Fig. 2)
900	Q, 1 h, 4 h (Fig. 3), 28 h
1000	Q (Fig. 3), 1 h, 4 h, 28 h
1100	Q, 1 h, 4 h (Fig. 4), 28 h (Fig. 4)
1200	Q, 1 h, 4 h (Fig. 4), 28 h (Fig. 4)
1300	Q, 4 h, 10 h (Fig. 5), 22 h (Fig. 5), 28 h, 40 h
1400	Q, 4 h, 10 h, 15 h (Fig. 5), 22 h
1500	Q, 1 h, 4 h, 10 h (Fig. 6), 15 h, 22 h (Fig. 6), 28 h
Zeolites X and LSX	
200	Q
300	Q
400	Q (Fig. 2), 4 h (Fig. 2)
800	2 h (Fig. 2)
900	4 h (Fig. 3)
1000	Q (Fig. 3)
1100	4 h (Fig. 4), 28 h (Fig. 4)
1200	4 h (Fig. 4), 28 h (Fig. 4)
1300	10 h (Fig. 5), 40 h (Fig. 5)
1400	15 h (Fig. 5)
1500	10 h (Fig. 6), 22 h (Fig. 6)
1550	24 h (Fig. 6)

[a] Q means that the sample was heated at a rate of 10 °C/min up to the fixed temperature and subsequently quenched in air. In the other cases, the samples were heated at a rate of 10 °C/min up to the reported temperature, kept in this conditions for the reported time, and subsequently quenched in air.

Zeolites Ba–A, Ba–X and Ba–LSX were subjected to various thermal treatments in a Lenton furnace, which ensures stable temperature to within ±2 °C, using Al_2O_3 crucibles. The thermal treatments, which are summarised in Table 1, were performed as follows. In some cases, the samples were heated at a rate of 10 °C/min up to the fixed temperature and subsequently quenched in air. In the other cases, the samples were heated at a rate of 10 °C/min up to the fixed temperature, kept in this conditions for the fixed time, and subsequently quenched in air.

These products were characterised by X-ray diffraction at room temperature using a Philips X'PERT diffractometer, Cu K_α radiation, collection of data between 20 and 40° 2θ with a step width of 0.02° 2θ and 1 s data collection per step.

Zeolites Ba–A, Ba–X and Ba–LSX were also characterised by simultaneous differential thermal analysis (DTA) and thermogravimetric analysis (TGA), using a Netzsch thermoanalyser model STA 409, α-Al_2O_3 as reference, and a 10 °C/min heating rate.

In addition to the thermal treatments summarized in Table 1, zeolites Ba–A, Ba–X, and Ba–LSX were thermally treated at 950 °C for 2 h in order to obtain the thermal collapse of the microporous zeolite structure and its irreversible dehydration. These thermally treated samples were chemically dissolved in the same previous acid solution and its Na^+ and K^+ (in the case of zeolite Ba–LSX) concentration were measured according to the procedure previously described in order to determine the Na and K (in the case of zeolite Ba–LSX) content of the final product of the thermal treatments.

3. Results

3.1. Cation exchange

The equivalent fraction of Ba in zeolites Ba–A, Ba–X and Ba–LSX is 0.96, 0.98 and 0.98, respectively. Moreover their Na residual amount, which appears very hard to be further reduced, is 0.20, 0.10, and 0.09 meq/g, respectively, whereas K residual amount of zeolite Ba–LSX is 0.01 meq/g. These Na residual amounts result in a Na_2O content of 0.62, 0.52, and 0.37 wt.% in the final products of the thermal treatment of Ba-exchanged zeolites, respectively, whereas the residual K content of zeolite Ba–LSX results in a K_2O content of 0.07% in the final product of thermal treatments of zeolite Ba–LSX. Such values appear, from the point of view of ceramic materials, quite low. Nevertheless it is noteworthy that zeolite Ba–A exhibits a far higher (about double) alkaline cations residual content than zeolites Ba–X and Ba–LSX. This finding could be easily explained if one bears in mind that in a previous paper[3] it was shown that the sample of zeolite A used in this work occluded some

$NaAlO_2$ within its β-cages, similar to feldspathoid behaviour.[17] Moreover in the same paper[3] the amount of Na, whose presence could be reasonably ascribed to occluded $NaAlO_2$, was evaluated to be 0.12 meq/g. If one considers that such amount of Na cannot be practically removed from zeolite A framework, it is evident that the residual exchangeable Na content still present at the end of the exchange procedure (0.08 meq/g) is practically equal to the Na residual amount of zeolites Ba–X and Ba–LSX, within the limit of experimental error.

3.2. X-ray diffraction

Fig. 2 shows that Ba-exchange results in a reduction of the crystallinity of the structure of the three different zeolites. Such reduction appears dramatic for zeolite A, sensible for zeolite LSX and hardly detectable for zeolite X.

Fig. 3 shows that, when zeolite Ba–A is thermally treated at 200 °C for 2 h, the total thermal collapse of the microporous zeolite structure occurs, thus giving rise to a completely amorphous product (Fig. 3a). When zeolite Ba–A is heated up to 500 °C, monoclinic celsian nuclei, whose size was estimated to range between 19.4 and 27.3 nm,[9] may be found to crystallise in the amorphous matrix arising from the thermal collapse of the zeolite structure (Fig. 3b). Raising the temperature of the thermal treatment up to 800 °C does not result in an increase of the amount of crystallised monoclinic celsian, as it can be seen in the XRD pattern of zeolite Ba–A thermally treated at 800 °C for 28 h (Fig. 3c). In such XRD pattern no sensible increase of intensity of diffraction peaks that can be ascribed to monoclinic celsian with respect to the XRD pattern of zeolite Ba–A heated at 500 °C and then quenched in air may be detected, whereas the appearance of diffraction peaks that can be ascribed to hexacelsian may be recorded. Zeolite Ba–X and Ba–LSX undergo thermal collapse at temperatures far higher than zeolite Ba–A, thus exhibiting a far higher thermal stability. In particular the diffraction peaks that can be ascribed to the zeolitic structure are still present in the XRD patterns of samples heated at 800 °C and then quenched in air (Fig. 3d and g). Such peaks disappear only after a 2 h thermal treatment at 850 °C which gives rise to completely amorphous products, as it can be recorded in the XRD patterns reported in Fig. 3f and i. It must be said that an almost completely amorphous product occurs by thermally treating zeolite Ba–X at 800 °C for 4 h, whereas, subjecting zeolite Ba–LSX to this same thermal treatment, a product which still exhibits a residual

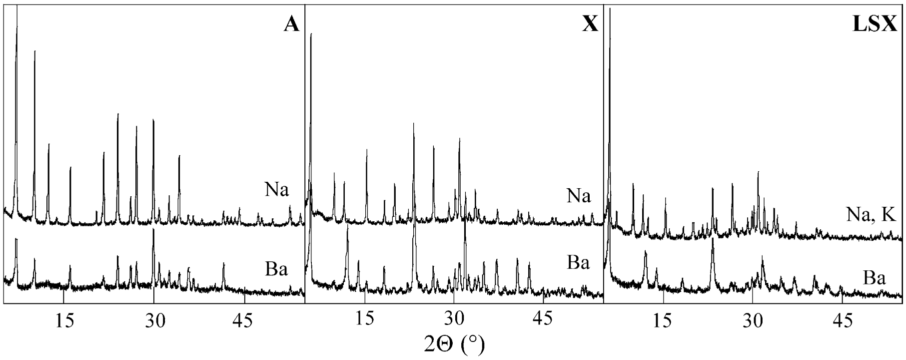

Fig. 2. XRD patterns of zeolites Na–A, Ba–A, Na–X, Ba–X, (Na, K)-LSX, and Ba–LSX.

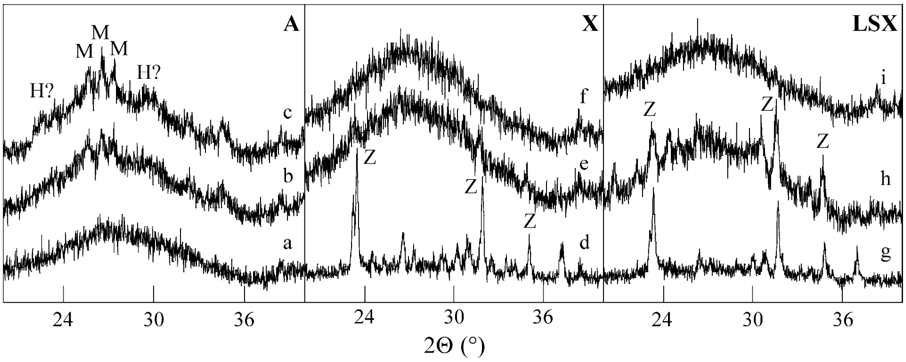

Fig. 3. XRD patterns of zeolite Ba–A thermally treated at 200 °C for 2 h (a), zeolite Ba–A heated at 500 °C and then quenched in air (b), zeolite Ba–A thermally treated at 800 °C for 28 h (c), zeolite Ba–X and Ba–LSX heated at 800 °C and then quenched in air (d and g, respectively), zeolite Ba–X and Ba–LSX thermally treated at 800 °C for 4 h (e and h, respectively), and zeolite Ba–X and Ba–LSX thermally treated at 850 for 2 h (f and i, respectively).

crystallinity is obtained. In Fig. 3 and in the following ones, the main diffraction peaks of monoclinic celsian, hexacelsian and zeolites are denoted with M, H, and Z, respectively.

In the XRD pattern of zeolite Ba–A thermally treated at 900 °C for 4 h (Fig. 4a) the same broad diffraction peaks ascribed to monoclinic celsian, which appeared in the XRD pattern of zeolite Ba–A heated at 500 °C and then quenched in air (Fig. 3b) and in the XRD pattern of zeolite Ba–A thermally treated at 800 °C for 28 h (Fig. 3c), appear together with the diffraction peaks of hexacelsian. It is noteworthy that, unlike the diffraction peaks of monoclinic celsian, whose intensity does not appear to increase with increasing temperature and time of thermal treatment in the temperature range 900–1000 °C, the intensity of diffraction peaks of hexacelsian is higher than the intensity of diffraction peaks of hexacelsian present in the XRD pattern of zeolite Ba–A thermally treated at 800 °C for 28 h (Fig. 3c). These same considerations may be repeated even for the XRD pattern of zeolite Ba–A heated at 1000 °C and then quenched in air (Fig. 4b). In the XRD pattern of zeolites Ba–X and Ba–LSX thermally treated at 900 °C for 4 h and heated at 1000 °C and then quenched in air no early crystallisation of nuclei of monoclinic celsian occurs in the amorphous phase arising from the thermal collapse of the microporous zeolitic structure. Actually in such XRD patterns only the diffraction peaks of hexacelsian may be recorded. It must also be noticed that the intensity of diffraction peaks of hexacelsian, which, of course, increases with increasing temperature, is higher in the XRD patterns of zeolite Ba–X than in the XRD patterns of zeolite Ba–LSX, ceteris paribus.

Thermal treatments of zeolite Ba–A at 1100 or 1200 °C (Fig. 5) give rise to an early crystallisation of hexacelsian followed by the conversion of hexacelsian into monoclinic celsian after prolonged heating (28 h). At 1200 °C the extent to which this conversion occurs is far greater than at 1100 °C, ceteris paribus. Even during the early stages of crystallisation of hexacelsian at 1100 or 1200 °C (the relevant XRD patterns are not reported), the presence of diffraction peaks of monoclinic celsian, similar to those reported in Figs. 3b and c, 4a and b, is recorded. Even thermal treatments of zeolites Ba–X and Ba–LSX at 1100 or 1200 °C give rise to an early crystallisation of hexacelsian followed by the conversion of hexacelsian into monoclinic celsian after prolonged heating (28 h). Nevertheless these phenomena strongly differ from those occurring after having performed the same thermal treatment on zeolite Ba–A. In particular the absence of nuclei of monoclinic celsian during the early stages of crystallisation of hexacelsian, typical of

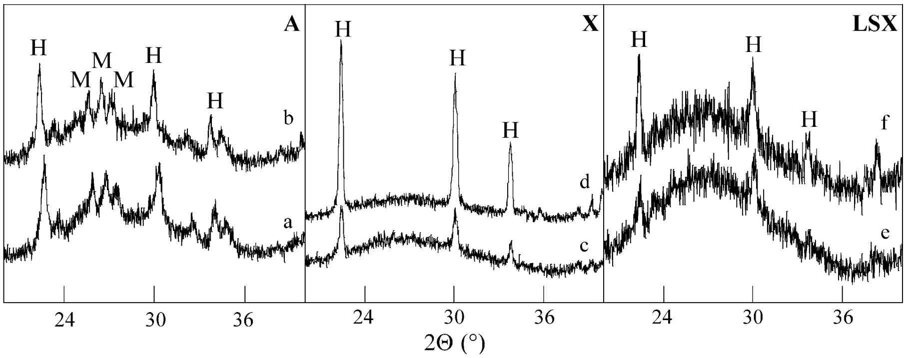

Fig. 4. XRD pattern of zeolites Ba–A, Ba–X and Ba–LSX thermally treated at 900 °C for 4 h (a, c, e, respectively) and heated at 1000 °C and then quenched in air (b, d, and f, respectively).

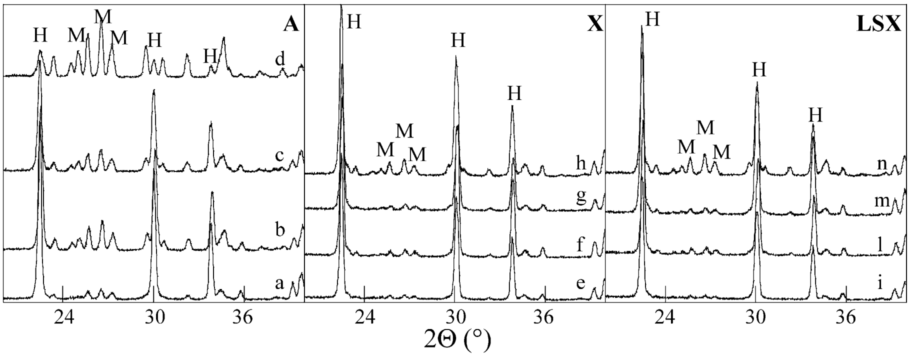

Fig. 5. XRD pattern of the following samples: zeolites Ba–A, Ba–X and Ba–LSX thermally treated at 1100 °C for 4 h (a, e, and i, respectively) and 28 h (b, f, l, respectively) and 1200 °C for 4 h (c, g, and m, respectively) and 28 h (d, h, and n, respectively).

zeolite Ba–A, is confirmed and the extent to which the conversion of hexacelsian to monoclinic celsian occurs is far lower thermally treating at 1100 or 1200 °C zeolites Ba–X and Ba–LSX rather than zeolite Ba–A, ceteris paribus.

Thermal treatments of zeolite Ba–A in the temperature range 1300–1400 °C (Fig. 6) give raise to the same sequence of transformations previously reported. It is noteworthy that the conversion of hexacelsian to monoclinic celsian attains completion at 1300 and 1400 °C at 22 and 15 h, respectively. Fig. 6 reports even the XRD pattern of zeolites Ba–X and Ba–LSX thermally treated at 1300 °C for 10 and 40 h and at 1400 °C for 15 h. The inspection of these XRD patterns reveals that the conversion of hexacelsian to monoclinic celsian starting from zeolites Ba–X and Ba–LSX is far slower than starting from zeolite Ba–A. In particular the following findings appear evident: (1) If the XRD patterns of zeolites Ba–A, Ba–X and Ba–LSX thermally treated at 1300 °C for 10 h are compared, the conversion of hexacelsian to monoclinic celsian appears almost completed starting from zeolite Ba–A, while its beginning can hardly be detected in the XRD patterns of zeolites Ba–X and Ba–LSX. (2) Starting from these zeolites, the completion of the conversion of hexacelsian to monoclinic celsian appears far from being attained in times equal (15 h at 1400 °C) or even far longer (40 h at 1300 °C) than the times necessary for the transformation of zeolite Ba–A into fully monoclinic celsian (15 h at 1400 °C, 22 h at 1300 °C).

The inspection of the XRD patterns of samples thermally treated at the highest temperatures (1500–1550 °C) of the investigated temperature range (Fig. 7) confirms the previous findings. In particular the full conversion of hexacelsian to monoclinic celsian (Fig. 7a and b) is attained thermally treating zeolite Ba–A at 1500 °C for 22 h. As far as zeolites Ba–X and Ba–LSX are concerned, the conversion of hexacelsian to monoclinic celsian is so slow that its completion is not attained even at temperatures (1550 °C) and times (24 h) higher than those necessary for the conversion of zeolite Ba–A into fully monoclinic celsian (22 h at 1500 °C).

3.3. Thermal analysis

In Fig. 8 the DTA and TGA curves of zeolites Ba–A, Ba–X and Ba–LSX are reported. In the three DTA curves a large low temperature endothermic effect and a sharp high temperature exothermic effect are evident. The low temperature endothermic effect can be ascribed to the progressive dehydration of zeolites. It must be said that the total water loss of zeolites Ba–X (21.0%)

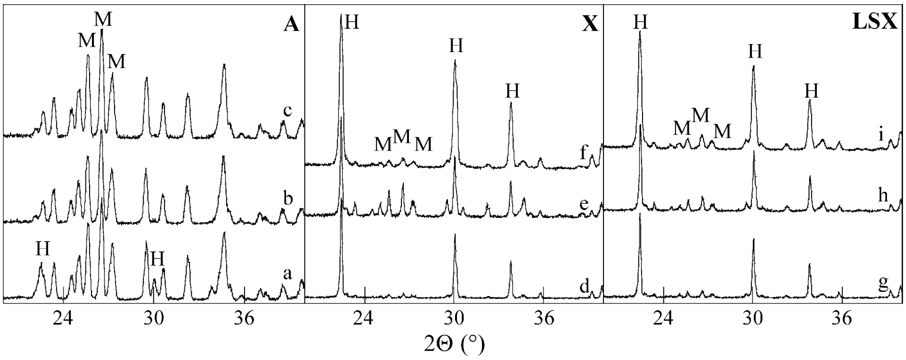

Fig. 6. XRD pattern of zeolite Ba–A thermally treated at 1300 °C for 10 (a) and 22 h (b) and at 1400 °C for 15 h (c), and zeolites Ba–X and Ba–LSX thermally treated at 1300 °C for 10 (d and g, respectively) and 40 h (e and h, respectively) and at 1400 °C for 15 h (f and i, respectively).

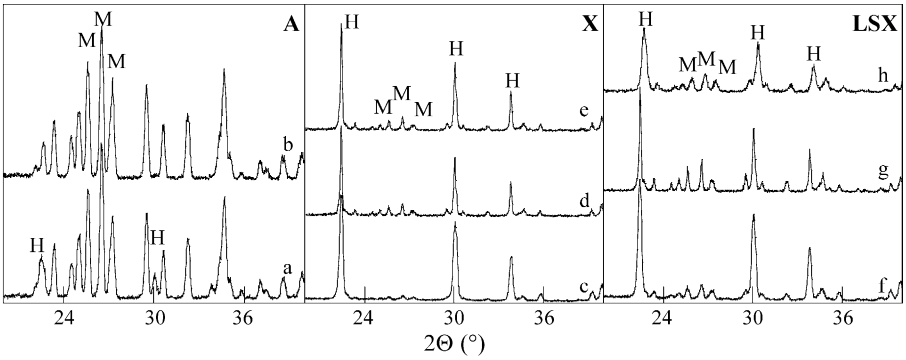

Fig. 7. XRD pattern of zeolite Ba–A thermally treated at 1500 °C for 10 (a) and 22 h (b), and zeolites Ba–X and Ba–LSX thermally treated at 1500 °C for 10 (c and f, respectively) and 22 h (d and g, respectively), and at 1550 °C for 24 h (e and h, respectively).

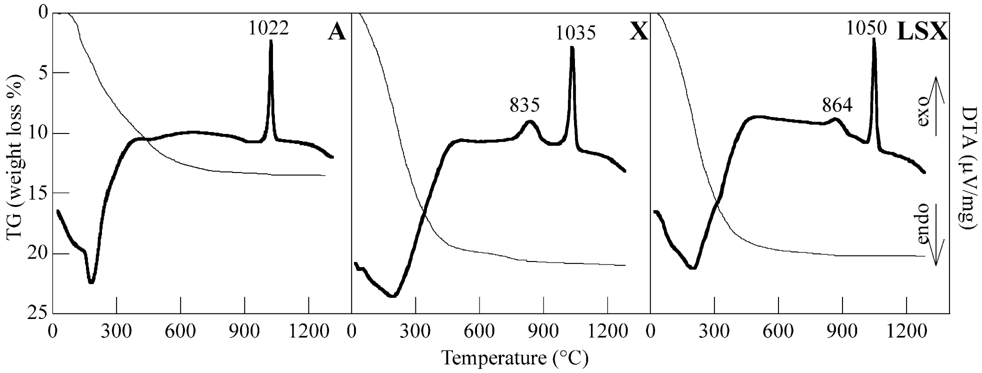

Fig. 8. DTA and TGA curves of zeolites Ba–A, Ba–X, and Ba–LSX.

and Ba–LSX (20.2%) is far higher than the one of zeolite Ba–A (13.5%). This finding could be reasonably ascribed to the fact that more void space is available for water molecules in Ba–X and Ba–LSX zeolites (framework density = 13.3×10^{21} T cm^{-3}, T = Si, Al atoms exhibiting tetrahedral coordination)[15] than in zeolite Ba–A (framework density = 14.2×10^{21} T cm^{-3}).[15] The sharp high temperature exothermic effect is related to the crystallisation of hexacelsian from the amorphous phase.

The temperatures at which the sharp exothermic effect is recorded (1022, 1035, and 1050 °C, for zeolites Ba–A, Ba–X and Ba–LSX, respectively) appear to be consistent with the XRD data. Actually, the presence of hexacelsian begins to be hardly detected after 1 h of thermal treatment at 900 °C starting from zeolite Ba–A (the XRD pattern is not reported), and after 4 h of thermal treatment at 900 °C starting from zeolites Ba–X and Ba–LSX. The difference between these temperatures is sufficiently accounted for by the fact that the former values were recorded in dynamic conditions whereas the latter value in static conditions.

Then in the DTA curves of zeolites Ba–X and Ba–LSX a small, broad exothermic effect is recorded at 837 and 864 °C, respectively. No evidence of the sluggish hexacelsian→monoclinic celsian transition is noted in the DTA curve of the three zeolite samples.

4. Discussion

On Ba exchange, zeolite A undergoes a framework distortion and a subsequent loss of crystallinity to a larger extent than zeolites X and LSX. This fact reflects also into their different thermal stability. Actually Ba exchange, which was found to give rise to a disrupting action even on other zeolite frameworks,[18–20] seems to make the framework of zeolite A far more prone to thermal collapse than zeolites X and LSX. In particular thermal collapse of the microporous zeolite structure was found to occur after a 2 h thermal treatment at 200 °C for zeolite A, after a 4 h thermal treatment at 800 °C for zeolite Ba–X, and after a 2 h thermal treatment at 850 °C for zeolite Ba–LSX. Evidence of the thermal breakdown of the structure of zeolites Ba–X and Ba–LSX could be found in their DTA curves. Actually it appears reasonable to relate the small, broad exothermic effect recorded at 837 and 864 °C, for zeolite Ba–X and Ba–LSX, respectively, to the final breakdown of their almost completely dehydrated microporous zeolitic structure with the consequent formation of more compact, amorphous phases. The difference between the temperatures recorded (800 °C in static conditions and 837 °C in dynamic conditions for zeolite Ba–X, 850 °C in static conditions and 864 °C in dynamic conditions for zeolite Ba–LSX) is sufficiently accounted for by the different conditions in which they were recorded. This interpretation is in agreement with Weidenthaler and Schmidt,[21] Trigueiro and coworkers,[22] and Chandrasekhar and Pramada.[23,24] These authors recorded a similar exothermic effect in the DTA curves of many different cation forms of zeolites A, X and Y and ascribed it to the thermal breakdown of their microporous structure.

Also the amorphous phase arising from the thermal collapse of the microporous structure of zeolite Ba–A exhibits a thermal behaviour which strongly differs from the thermal behaviour of the amorphous phase arising from the thermal collapse of zeolites Ba–X and Ba–LSX. The crucial point in which such thermal behaviours differ from each other is the fact that, starting from 500 °C, the presence of nuclei of monoclinic celsian dispersed in the amorphous matrix arising from the thermal collapse of the microporous structure of zeolite Ba–A is recorded prior to the crystallisation of hexacelsian. This phenomenon was explained as follows. The framework of the various zeolites is made up of basic TO_4 (T = Si, Al) tetrahedra, which are the primary building units in every aluminosilicate. These basic TO_4 (T = Si, Al) tetrahedra may be thought to be assembled in zeolites in such a way to form slightly more complex units, called secondary building units (SBU).[15] When the thermal breakdown occurs, the long range order of the microporous zeolite structure is destroyed, thus giving rise to an amorphous phase. Nevertheless the association of some of the basic TO_4 tetrahedra in SBUs, which was reported either in glass[25,26] or melts,[27,28] was detected even in the amorphous phase arising from the thermal collapse of the microporous structure of zeolite Ba–A.[8] In particular the use of the FTIR spectroscopy allowed to reveal the presence of the secondary building units of zeolite A in such amorphous phase and that thermal treatments in the temperature range 200–400 °C resulted in a middle-range order which favoured the crystallization of nuclei of monoclinic celsian at 500 °C.[8] The further evolution of the amorphous phase in the 500–800 °C range of thermal treatment instead of promoting the crystalline growth of monoclinic celsian, created a middle-range order favourable to the crystallisation of hexacelsian starting from 900 °C. Nevertheless the presence of the nuclei of monoclinic celsian previously formed appears of crucial importance as they were found to favour the conversion of hexacelsian into monoclinic celsian at temperatures far lower than those reported in the literature.[2]

Unlike the amorphous phase arising from the thermal collapse of the microporous structure of zeolite Ba–A, the amorphous phase arising from the thermal collapse of microporous structure of zeolite Ba–X and Ba–LSX does not give rise to the crystallisation of nuclei of monoclinic celsian prior to the crystallisation of hexacelsian. A possible explanation of this finding could be related to the higher thermal stability of zeolites Ba–X and Ba–LSX. Actually the crystallization of nuclei of monoclinic celsian at 500 °C in the amorphous phase arising from the thermal collapse of zeolite Ba–A is favoured by the middle-range order resulting from the thermal treatments in the temperature range 200–400 °C.[8] These phenomena are very unlikely to occur for zeolites Ba–X and Ba–LSX on account of the following reasons: (1) Zeolites Ba–X and Ba–LSX exhibits good thermal stability in the temperature range 200–500 °C; (2) At the temperatures at which the thermal collapse of zeolites Ba–X and Ba–LSX occurs (about 800–850 °C) a middle-range order favourable to the crystallisation of hexacelsian is created.[8] The immediate consequence of the fact that the thermal collapse of the microporous structure of zeolites Ba–X and Ba–LSX does not give rise to the crystallisation of small nuclei of monoclinic celsian prior to the crystallisation of hexacelsian is that the transformation of hexacelsian to monoclinic celsian, starting from zeolites Ba–X and Ba–LSX, occurs at temperatures far higher and/or times far longer than starting from zeolite Ba–A. Such high temperatures and long times appear very similar to those reported in ref. 2 where the literature concerning the synthesis of celsian was reviewed. In particular in this study it was found that, starting from the samples of zeolite Ba–X and Ba–LSX of this work, the conversion of hexacelsian into monoclinic celsian does not attain completion even in the most severe experimental conditions experienced (1550 °C, 24 h). This last finding does not appear, at a first glance, in agreement with the results of refs. 2 and 14. Nevertheless this discrepancy may be easily explained considering that the higher reactivity of samples of zeolite Ba–X of refs. 2 and 14 than samples of zeolites Ba–X and Ba–LSX of this work appears related to their different residual Na content (zeolite Ba–X of refs. 2 and 14: 0.26 and 0.61 meq/g, respectively; zeolites Ba–X and Ba–LSX of this work: 0.10 and 0.09 meq/g, respectively). Thus the role played by Na, whose presence was found to result in lower temperatures and times of crystallisation of monoclinic celsian starting from zeolite Ba–A, ceteris paribus,[3] is confirmed even for zeolite Ba–X.

5. Conclusions

This investigations supplied new insight into the thermal transformation of Ba-exchanged zeolites into celsian. First of all the mineralising role played by Na residual content, which was revealed in the thermal transformation of zeolite Ba–A into celsian,[3] was confirmed even for zeolites Ba–X and Ba–LSX.

Then an other point which appears worth to be stressed is the far greater reactivity of zeolite Ba–A than zeolites Ba–X and Ba–LSX precursors. This finding appears very interesting inasmuch as the amorphous phases arising from the thermal collapse of the microporous structures of zeolites Ba–A and Ba–LSX exhibit a chemical composition extremely close to each other and, in particular, exhibit about the same Si/Al ratio. Moreover the amorphous phases arising from the thermal collapse of the microporous structure of zeolites Ba–X and Ba–LSX, despite the different chemical composition, behave in very similar ways as far as their subsequent thermal transformations are concerned. These considerations evidence the fact that the middle-range order of the amorphous phase arising from the thermal collapse of the microporous zeolitic structure greatly affects the reactivity of the system, unlike its Si/Al ratio. Such middle-range order could be affected by the structure of the zeolite from which the amorphous phase originated and by the thermal stability of the zeolitic structure itself. Actually the former could affect the middle-range order of the amorphous phase as different zeolites, when they undergo thermal breakdown, could give rise to amorphous phases in which different amounts of the various SBUs are dispersed.[25–28] The latter could play an equivalent role as an high thermal stability of the zeolitic structure may inhibit the occurrence of the low temperature (200–400 °C) transformations in the amorphous phase.[8]

Acknowledgements

This work was carried out with the financial contribution of the Ministry of University and Scientific and Technological Research.

References

1. Talmy, I. G., Haught, D. A. and Wuchina, E. J., Ceramics in the system $BaO\cdot Al_2O_3\cdot 2SiO_2$–$SrO\cdot Al_2O_3\cdot 2SiO_2$ (BAS-SAS): polymorphism, processing and properties. In *Proceedings of the 6th International SAMPE Electronic Conference*, ed. A. B. Goldberg and C. A. Harper. Society for the Advancement of Materials and Process Engineering, Covina, CA, USA, 1992, pp. 687–698.
2. Dell'Agli, G., Ferone, C., Mascolo, M. C. and Pansini, M., Thermal transformation of Ba-exchanged A and X zeolites into monoclinic celsian. *Solid State Ionics*, 2000, **127**, 309–317.
3. Ferone, C., Dell'Agli, G., Mascolo, M. C. and Pansini, M., New insight into the thermal transformation of barium-exchanged zeolite A to celsian. *Chem. Mat.*, 2002, **14**, 797–803.
4. Debsikdar, J. C., Gel to Glass conversion and crystallization of alkoxy-derived barium aluminosilicate gel. *J. Non-Cryst. Sol.*, 1992, **144**, 269–276.
5. Talmy, I. G. and Haught, D. A., *Low Temperature Synthesis of High Purity Monoclinic Celsian*. US Patent 5,041,400, 20 Aug, 1991.
6. Chen, M., Lee, W. E. and James, P. F., Preparation and characterisation of alkoxide-derived celsian glass-ceramic. *J. Non-Cryst. Solids*, 1991, **130**, 322–325.
7. Lin, H. C. and Foster, W. R., Studies in the system BaO–Al_2O_3–SiO_2 I. The polymorphism of celsian. *Am. Mineral.*, 1962, **53**, 134–144.
8. Aronne, A., Esposito, S., Ferone, C., Pansini, M. and Pernice, P., FTir study of the thermal transformation of barium-exchanged zeolite A to celsian. *J. Mater. Chem.*, 2002, **12**, 3039–3045.
9. Clayden, N. J., Esposito, S., Ferone, C. and Pansini, M., ^{29}Si and ^{27}Al NMR study of the thermal transformation of barium exchanged zeolite A to celsian. *J. Mat. Chem.*, 2003, **13**, 1681–1685.
10. Subramanian, M. A., Corbin, D. and Farlan, R. D., X-ray and mass NMR characterization of the thermal transformation of Li(Na)-Y zeolite to lithium aluminosilicates. *Mat. Res. Bull.*, 1986, **21**, 1525–1532.
11. Chowdry, U. V., Corbin, D. R. and Subramanian, M. A., *Anorthite-Cordierite Based Ceramics from Zeolites*. US Patent 4,813,303, 21 March, 1989.
12. Subramanian, M. A., Corbin, D. R. and Chowdry, U. V., Zeolites as precursors to aluminosilicates based ceramics for microelectronic packaging. *Adv. Ceram.*, 1989, **26**, 239–247.
13. Corbin, D. R., Parise, J. B., Chowdry, U. V. and Subramanian, M. A., Designing zeolites as novel precursors to electronic ceramics. *Mater. Res. Symp. Proc.*, 1991, **233**, 213–217.
14. Hoghooghi, B., McKittrick, J., Helsel, E. and Lopez, O., Microstructural development, densification, and hot pressing of celsian ceramics from ion-exchanged zeolite precursors. *J. Am. Ceram. Soc.*, 1998, **81**, 845–852.
15. Baerlocher, C., Meier, W. M. and Olson, D. H., *Atlas of the Zeolite Framework Types*. Elsevier, Amsterdam, 2001.
16. Schwarzenbach, G. and Flaschka, H., *Complexometric Titration*. Methuen, London, 1969.
17. Breck, D. W., *Zeolite Molecular Sieves: Structure, Chemistry and Use*. Wiley, New York, NY, 1974.
18. Barrer, R. M. and Munday, B. M., Cation exchange reactions of a sedimentary phillipsite. *J. Chem. Soc. A*, 1971, 2904–2909.
19. Colantuono, A., Dal Vecchio, S., Mascolo, G. and Pansini, M., Dilatometric behaviour of habazite. *J. Therm. Anal.*, 1996, **47**, 281–289.
20. Passaglia, E., Natural zeolites. In *Occurrence, Properties, Uses, Lattice-Constant Variations in Cation-Exchanged Chabazites*, ed. L. B. Sand and F. A. Mumpton. Pergamon Press, Elmsford, 1976, pp. 45–52.
21. Weidenthaler, C. and Schmidt, W., Thermal stability and thermal transformations of Co^{2+}- or Ni^{2+}-exchanged zeolites A, X, and Y. *Chem. Mat.*, 2000, **12**, 3811–3820.
22. Trigueiro, F. E., Monteiro, D. F. J., Zotin, F. M. Z. and Falabella Sousa-Aguiar, E., Thermal stability of Y zeolites containing different rare earth cations. *Journal of Alloys and Compounds*, 2002, **344**, 337–341.
23. Chandrasekhar, S. and Pramada, P. N., Sintering behaviour of calcium exchanged low silica zeolites synthesized from kaolin. *Ceramics International*, 2001, **27**, 105–114.
24. Chandrasekhar, S. and Pramada, P. N., Thermal studies of low silica zeolites and their magnesium exchanged forms. *Ceramics International*, 2002, **28**, 177–186.
25. De Jong, B. H. W. S., Schramm, C. M. and Parziale, V. E., Polymerization of silicate and aluminate tetrahedra in glasses, melts, and aqueous solutions. V. The polymeric structure of silica in albite and anorthite composition glass and the devitrification of amorphous anorthite. *Geochim. Cosmochim. Acta*, 1984, **48**, 2619–2629.
26. Dimijtrievic, R., Dondur, V. and Kremenovic, A., Thermally induced phase transformations of Ca-exchanged LTA and FAU zeolite frameworks: Rietveld refinement of the hexagonal $CaAl_2Si_2O_8$ diphyllosilicate structure. *Zeolites*, 1996, **16**, 294–300.
27. Kirkpatrick, R., Theory of nucleation in silicate melts. *Am. Mineral.*, 1983, **68**, 66–77.
28. Seifert, F., Mysen, B. and Virgo, D., Three-dimensional network structure of quenched melts (glass) in the systems SiO_2–$NaAlO_2$, SiO_2–$CaAl_2O_4$ and SiO_2–$MgAl_2O_4$. *Am. Mineral.*, 1982, **67**, 696–717.